

This article was downloaded by:

On: 23 January 2011

Access details: *Access Details: Free Access*

Publisher *Taylor & Francis*

Informa Ltd Registered in England and Wales Registered Number: 1072954 Registered office: Mortimer House, 37-41 Mortimer Street, London W1T 3JH, UK



## Journal of Coordination Chemistry

Publication details, including instructions for authors and subscription information:

<http://www.informaworld.com/smpp/title~content=t713455674>

### Hydrothermal assembly and structural characterization of an unprecedented one-dimensional chain constructed from nickel diphosphopentamolybdate clusters

Q. B. Bo<sup>a</sup>; Z. X. Sun<sup>a</sup>; G. X. Sun<sup>a</sup>; Z. W. Zhang<sup>a</sup>; C. L. Chen<sup>a</sup>; Y. X. Li<sup>a</sup>

<sup>a</sup> Institute of Chemistry and Chemical Engineering, Jinan University, Jinan, Shandong 250022, P.R. China

**To cite this Article** Bo, Q. B. , Sun, Z. X. , Sun, G. X. , Zhang, Z. W. , Chen, C. L. and Li, Y. X.(2007) 'Hydrothermal assembly and structural characterization of an unprecedented one-dimensional chain constructed from nickel diphosphopentamolybdate clusters', *Journal of Coordination Chemistry*, 60: 3, 275 – 283

**To link to this Article:** DOI: 10.1080/00958970600763607

**URL:** <http://dx.doi.org/10.1080/00958970600763607>

PLEASE SCROLL DOWN FOR ARTICLE

Full terms and conditions of use: <http://www.informaworld.com/terms-and-conditions-of-access.pdf>

This article may be used for research, teaching and private study purposes. Any substantial or systematic reproduction, re-distribution, re-selling, loan or sub-licensing, systematic supply or distribution in any form to anyone is expressly forbidden.

The publisher does not give any warranty express or implied or make any representation that the contents will be complete or accurate or up to date. The accuracy of any instructions, formulae and drug doses should be independently verified with primary sources. The publisher shall not be liable for any loss, actions, claims, proceedings, demand or costs or damages whatsoever or howsoever caused arising directly or indirectly in connection with or arising out of the use of this material.

## Hydrothermal assembly and structural characterization of an unprecedented one-dimensional chain constructed from nickel diphosphomolybdate clusters

Q. B. BO\*, Z. X. SUN, G. X. SUN, Z. W. ZHANG, C. L. CHEN and Y. X. LI

Institute of Chemistry and Chemical Engineering, Jinan University,  
106, Jiwei Road, Jinan, Shandong 250022, P.R. China

(Received in final form 24 February 2006)

A novel molybdenum phosphate complex,  $[\text{Ni}(1)(\text{en})_2(\text{PO}_4)_2\text{Mo}_5\text{O}_{15}][\text{Ni}(2)(\text{en})_2(\text{H}_2\text{O})_2] \cdot \text{H}_2\text{en} \cdot 3\text{H}_2\text{O}$  (**1**), has been synthesized under hydrothermal conditions. The complex was characterized by elemental analysis, FT-IR, DTA/TG and single crystal X-ray diffraction. The compound is orthorhombic, space group  $P2_12_12_1$ , with  $a = 12.580(3)$ ,  $b = 17.676(4)$ ,  $c = 17.969(4)$  Å,  $V = 3995.5(15)$  Å<sup>3</sup>,  $Z = 4$ , and was refined to  $R_1 = 0.0301$ ,  $wR_2 = 0.0715$ . It possesses an unprecedented one-dimensional chain structure constructed from molybdenum phosphate clusters and nickel complex fragments.

**Keywords:** Nickel; Phosphomolybdate; Hybrid compound; Hydrothermal synthesis; Crystal structure

### 1. Introduction

Polyoxoanions have attracted much attention due to their potential application in catalysis, electronic conductivity, magnetism, medicine, and optical materials. Of the various polyoxoanions, a new class of materials based on anionic molybdenum phosphate frameworks has received much attention [1–3]. As a result, some molybdenum phosphates have been studied [4–6]. Here we report a novel compound, **1**, which exhibits a one-dimensional chain constructed by  $[(\text{PO}_4)_2\text{Mo}_5\text{O}_{15}]^{6-}$  units covalently linked *via*  $[\text{Ni}(\text{en})_2\text{O}_2]^{2+}$  ions. Its thermal stability and FT-IR spectra have been studied.

### 2. Experimental

#### 2.1. Synthesis

Reagents were purchased commercially and used without further purification. CHN analyses were carried out on a Perkin-Elmer 2400 Series II CHNS/O system and ICP

\*Corresponding author. Email: chm\_boqb@ujn.edu.cn

Table 1. Crystallographic parameters and refinement details for **1**.

Empirical formula	C <sub>10</sub> H <sub>52</sub> Mo <sub>5</sub> N <sub>10</sub> Ni <sub>2</sub> O <sub>28</sub> P <sub>2</sub>
Formula weight	1419.68
Crystal system	Orthorhombic
Space group	<i>P</i> 2 <sub>1</sub> 2 <sub>1</sub>
<i>a</i> (Å)	12.580(3)
<i>b</i> (Å)	17.676(4)
<i>c</i> (Å)	17.969(4)
$\alpha$ (°)	90
$\beta$ (°)	90
$\gamma$ (°)	90
<i>V</i> (Å <sup>3</sup> )	3995.5(15)
<i>Z</i>	4
<i>D</i> <sub>Calcd</sub> (g cm <sup>-3</sup> )	2.360
$\mu$ (mm <sup>-1</sup> )	2.624
Reflections collected	20984
Independent reflections	7027 [ <i>R</i> (int) = 0.0574]
Final <i>R</i> indices [ <i>I</i> > 2 $\sigma$ ( <i>I</i> )]	<i>R</i> <sub>1</sub> = 0.0301, <i>wR</i> <sub>2</sub> = 0.0715
<i>R</i> indices (all data)	<i>R</i> <sub>1</sub> = 0.0330, <i>wR</i> <sub>2</sub> = 0.0734

Table 2. Selected bond distances (Å) for **1**.

Mo(1)–O(14)	1.709(5)	Mo(3)–O(6)	2.362(4)	Ni(2)–O(25)	2.141(5)
Mo(1)–O(15)	1.720(4)	Mo(4)–O(21)	1.704(5)	O(1)–P(1)	1.564(4)
Mo(1)–O(13)	1.924(4)	Mo(4)–O(20)	1.721(4)	O(2)–P(1)	1.528(4)
Mo(1)–O(9)	1.931(4)	Mo(4)–O(11)	1.919(4)	O(3)–P(1)	1.555(4)
Mo(1)–O(5)	2.251(4)	Mo(4)–O(12)	1.920(4)	O(4)–P(1)	1.524(4)
Mo(1)–O(1)	2.309(4)	Mo(4)–O(7)	2.145(4)	O(5)–P(2)	1.552(4)
Mo(2)–O(16)	1.712(5)	Mo(4)–O(3)	2.478(4)	O(6)–P(2)	1.551(4)
Mo(2)–O(17)	1.713(4)	Mo(5)–O(22)	1.699(5)	O(7)–P(2)	1.516(5)
Mo(2)–O(10)	1.926(4)	Mo(5)–O(23)	1.724(4)	O(8)–P(2)	1.524(4)
Mo(2)–O(9)	1.948(4)	Mo(5)–O(13)	1.911(4)	N(1)–Ni(1)	2.088(5)
Mo(2)–O(6)	2.201(4)	Mo(5)–O(12)	1.927(5)	N(2)–Ni(1)	2.085(6)
Mo(2)–O(1)	2.358(4)	Mo(5)–O(3)	2.162(4)	N(3)–Ni(1)	2.113(6)
Mo(3)–O(18)	1.706(4)	Mo(5)–O(5)	2.348(4)	N(4)–Ni(1)	2.083(6)
Mo(3)–O(19)	1.717(4)	Ni(1)–O(8)#1	2.090(4)	N(5)–Ni(2)	2.088(6)
Mo(3)–O(10)	1.912(4)	Ni(1)–O(4)	2.198(4)	N(6)–Ni(2)	2.096(6)
Mo(3)–O(11)	1.947(4)	O(8)–Ni(1)#2	2.090(4)	N(7)–Ni(2)	2.108(6)
Mo(3)–O(2)	2.233(4)	Ni(2)–O(24)	2.090(5)	N(8)–Ni(2)	2.075(6)

Symmetry transformations used to generate equivalent atoms are #1:  $-x + 3/2, -y + 1, z - 1/2$ ; #2:  $-x + 3/2, -y + 1, z + 1/2$ .

analyses (Ni, P, Mo) on a Perkin-Elmer Optima 3300DV spectrometer. FT-IR spectra (CsI pellets) were measured on a Perkin-Elmer spectrophotometer in the 4000–200 cm<sup>-1</sup> region. The thermal stability of **1** was examined using a Perkin-Elmer Diamond TG/DTA instrument. Compound **1** was prepared hydrothermally from a mixture of NiSO<sub>4</sub>·6H<sub>2</sub>O, (NH<sub>4</sub>)<sub>6</sub>Mo<sub>7</sub>O<sub>24</sub>·6H<sub>2</sub>O, H<sub>3</sub>PO<sub>4</sub>, en and H<sub>2</sub>O at a mol ratio of 2:5:10:12:550, heated in a Teflon-lined stainless steel autoclave at 160°C for 36 h under static conditions and a fill volume of 75%. After cooling the reaction mixture to room temperature, the blue-green block-like crystals that had formed were separated and washed repeatedly with distilled water and ethanol. The crystals were dried in air at room temperature. The average size of the crystals was about 3 mm across, and no other solid phase was found in the final product. Anal. Calcd for C<sub>10</sub>H<sub>52</sub>Mo<sub>5</sub>N<sub>10</sub>Ni<sub>2</sub>O<sub>28</sub>P<sub>2</sub> (%): C, 8.52; H, 3.65; N, 9.93; Ni, 8.31; P, 4.44; Mo, 33.94. Found: C, 8.46; H, 3.69; N, 9.87; Ni, 8.27; P, 4.36; Mo, 33.79.

Table 3. Selected bond angles (deg) for **1**.

Angle	(deg)	Angle	(deg)	Angle	(deg)
O(14)–Mo(1)–O(15)	104.2(2)	O(10)–Mo(3)–O(6)	69.64(16)	N(1)–Ni(1)–O(4)	90.16(19)
O(14)–Mo(1)–O(13)	98.7(2)	O(11)–Mo(3)–O(6)	86.63(16)	O(8)#1–Ni(1)–O(4)	85.54(16)
O(15)–Mo(1)–O(13)	101.2(2)	O(2)–Mo(3)–O(6)	87.26(14)	N(3)–Ni(1)–O(4)	174.4(2)
O(14)–Mo(1)–O(9)	100.4(2)	O(21)–Mo(4)–O(20)	100.3(2)	N(8)–Ni(2)–N(5)	177.3(2)
O(15)–Mo(1)–O(9)	99.2(2)	O(21)–Mo(4)–O(11)	101.5(2)	N(8)–Ni(2)–O(24)	89.2(2)
O(13)–Mo(1)–O(9)	147.66(18)	O(20)–Mo(4)–O(11)	97.9(2)	N(5)–Ni(2)–O(24)	92.7(2)
O(14)–Mo(1)–O(5)	168.40(19)	O(21)–Mo(4)–O(12)	105.6(2)	N(8)–Ni(2)–N(6)	99.7(2)
O(15)–Mo(1)–O(5)	86.3(2)	O(20)–Mo(4)–O(12)	97.5(2)	N(5)–Ni(2)–N(6)	82.3(2)
O(13)–Mo(1)–O(5)	73.99(17)	O(11)–Mo(4)–O(12)	145.68(18)	O(24)–Ni(2)–N(6)	88.8(2)
O(9)–Mo(1)–O(5)	82.60(17)	O(21)–Mo(4)–O(7)	87.7(2)	N(8)–Ni(2)–N(7)	82.1(2)
O(14)–Mo(1)–O(1)	90.63(18)	O(20)–Mo(4)–O(7)	171.9(2)	N(5)–Ni(2)–N(7)	95.9(2)
O(15)–Mo(1)–O(1)	164.59(19)	O(11)–Mo(4)–O(7)	81.25(17)	O(11)–O(1)–Ni(2)	90.0(2)
O(13)–Mo(1)–O(1)	80.41(16)	O(12)–Mo(4)–O(7)	79.21(17)	N(6)–Ni(2)–N(7)	177.8(2)
O(9)–Mo(1)–O(1)	73.51(16)	O(21)–Mo(4)–O(3)	172.4(2)	N(8)–Ni(2)–O(25)	90.0(2)
O(5)–Mo(1)–O(1)	79.41(14)	O(20)–Mo(4)–O(3)	84.72(19)	N(5)–Ni(2)–O(25)	88.1(3)
O(16)–Mo(2)–O(17)	103.5(2)	O(11)–Mo(4)–O(3)	83.32(15)	O(24)–Ni(2)–O(25)	178.8(2)
O(16)–Mo(2)–O(10)	97.6(2)	O(12)–Mo(4)–O(3)	67.83(16)	N(6)–Ni(2)–O(25)	90.4(3)
O(17)–Mo(2)–O(10)	99.4(2)	O(7)–Mo(4)–O(3)	87.14(15)	N(7)–Ni(2)–O(25)	90.8(2)
O(16)–Mo(2)–O(9)	101.2(2)	O(22)–Mo(5)–O(23)	103.8(2)	P(1)–O(1)–Mo(1)	127.6(2)
O(17)–Mo(2)–O(9)	95.3(2)	O(22)–Mo(5)–O(13)	98.5(2)	O(22)–O(1)–Mo(2)	128.8(2)
O(10)–Mo(2)–O(9)	152.67(19)	O(23)–Mo(5)–O(13)	99.7(2)	Mo(1)–O(1)–Mo(2)	92.92(14)
O(16)–Mo(2)–O(6)	156.9(2)	O(22)–Mo(5)–O(12)	99.3(2)	P(1)–O(2)–Mo(3)	125.6(2)
O(17)–Mo(2)–O(6)	99.0(2)	O(23)–Mo(5)–O(12)	94.1(2)	P(1)–O(3)–Mo(5)	129.2(2)
O(10)–Mo(2)–O(6)	73.14(16)	O(13)–Mo(5)–O(12)	154.09(18)	P(1)–O(3)–Mo(4)	134.8(2)
O(9)–Mo(2)–O(6)	81.91(17)	O(22)–Mo(5)–O(3)	96.0(2)	Mo(5)–O(3)–Mo(4)	93.37(15)
O(16)–Mo(2)–O(1)	85.80(19)	O(23)–Mo(5)–O(3)	158.86(18)	P(1)–O(4)–Ni(1)	135.8(3)
O(17)–Mo(2)–O(1)	165.75(18)	O(13)–Mo(5)–O(3)	84.56(17)	P(2)–O(5)–Mo(1)	127.2(2)
O(10)–Mo(2)–O(1)	89.86(15)	O(12)–Mo(5)–O(3)	75.03(17)	P(2)–O(5)–Mo(5)	129.3(3)
O(9)–Mo(2)–O(1)	72.08(16)	O(22)–Mo(5)–O(5)	166.8(2)	Mo(1)–O(5)–Mo(5)	93.02(14)
O(6)–Mo(2)–O(1)	73.24(14)	O(23)–Mo(5)–O(5)	87.10(18)	P(2)–O(6)–Mo(2)	130.9(2)
O(18)–Mo(3)–O(19)	102.2(2)	O(13)–Mo(5)–O(5)	71.92(16)	P(2)–O(6)–Mo(3)	132.7(2)
O(18)–Mo(3)–O(10)	100.1(2)	O(12)–Mo(5)–O(5)	87.13(17)	Mo(2)–O(6)–Mo(3)	94.57(14)
O(19)–Mo(3)–O(10)	101.4(2)	O(3)–Mo(5)–O(5)	74.46(14)	P(2)–O(7)–Mo(4)	127.9(2)
O(18)–Mo(3)–O(11)	101.2(2)	N(4)–Ni(1)–O(8)#1	93.1(2)	P(2)–O(8)–Ni(1)#2	130.7(2)
O(19)–Mo(3)–O(11)	96.5(2)	N(2)–Ni(1)–O(8)#1	89.48(19)	Mo(1)–O(9)–Mo(2)	121.4(2)
O(10)–Mo(3)–O(11)	148.59(18)	N(1)–Ni(1)–O(8)#1	170.4(2)	Mo(3)–O(10)–Mo(2)	121.9(2)
O(18)–Mo(3)–O(2)	85.94(19)	N(4)–Ni(1)–N(3)	81.3(2)	Mo(4)–O(11)–Mo(3)	145.7(2)
O(19)–Mo(3)–O(2)	171.84(18)	N(2)–Ni(1)–N(3)	93.2(3)	Mo(4)–O(12)–Mo(5)	123.1(2)
O(10)–Mo(3)–O(2)	78.00(17)	N(1)–Ni(1)–N(3)	92.3(2)	Mo(5)–O(13)–Mo(1)	120.9(2)

Symmetry transformations used to generate equivalent atoms are #1:  $-x + 3/2, -y + 1, z - 1/2$ ; #2:  $-x + 3/2, -y + 1, z + 1/2$ .

## 2.2. Crystallography

A crystal fragment of dimensions of  $0.49 \times 0.47 \times 0.43$  mm was selected under an optical microscope and glued to a thin glass fibre with epoxy resin. X-ray intensity data were measured at 293 K on a Bruker SMART APEX CCD-based diffractometer (Mo  $K\alpha$  radiation,  $\lambda = 0.71073$  Å). The raw frame data for the compound were integrated into SHELX-format reflection files and corrected for Lorentz and polarization effects using SAINT [7]. Corrections for incident and diffracted beam absorption effects were applied using SADABS [7]. Compound **1** crystallizes in the space group  $P2_12_12_1$ , as determined by systematic absences in the intensity data, intensity statistics and the successful solution and refinement of the structure. The structure was solved by a combination of direct methods and difference Fourier syntheses and refined against  $F^2$  by full-matrix least-squares techniques. Crystal data, data collection parameters,

Table 4. Atomic coordinates ( $\times 10^4$ ) and equivalent isotropic displacement parameters ( $\text{\AA}^2 \times 10^3$ ) for **1**.

Atom	$x/a$	$y/b$	$z/c$	$U(\text{eq})$	Atom	$x/a$	$y/b$	$z/c$	$U(\text{eq})$
Mo(1)	8309(1)	6097(1)	6536(1)	20(1)	O(13)	7141(3)	6616(2)	6071(2)	21(1)
Mo(2)	8764(1)	4228(1)	6278(1)	19(1)	O(14)	9311(4)	6411(3)	5973(3)	33(1)
Mo(3)	6442(1)	3391(1)	5874(1)	19(1)	O(15)	8457(4)	6613(2)	7340(2)	32(1)
Mo(4)	4368(1)	4778(1)	6381(1)	21(1)	O(16)	9732(4)	4364(3)	5621(3)	33(1)
Mo(5)	5710(1)	6437(1)	6380(1)	21(1)	O(17)	9362(4)	3651(3)	6918(2)	32(1)
N(1)	8030(5)	7103(3)	4587(3)	28(1)	O(18)	6144(4)	2818(2)	5138(3)	33(1)
N(2)	7009(6)	6826(3)	3267(3)	37(2)	O(19)	6376(4)	2774(3)	6611(3)	34(1)
N(3)	9420(5)	6636(3)	3288(3)	33(1)	O(20)	3652(4)	4957(3)	5584(2)	32(1)
N(4)	9312(5)	5617(3)	4430(3)	34(1)	O(21)	3396(4)	4413(3)	6934(3)	36(1)
N(5)	8647(5)	9227(3)	7217(3)	36(1)	O(22)	5078(4)	6959(3)	5721(3)	33(1)
N(6)	9105(5)	9157(3)	5721(3)	36(2)	O(23)	5670(4)	7003(2)	7161(2)	31(1)
N(7)	8908(5)	10980(3)	7217(3)	39(2)	O(24)	10630(4)	9993(3)	6639(2)	37(1)
N(8)	9284(5)	10956(3)	5710(3)	34(1)	O(25)	7326(4)	10167(3)	6233(4)	51(2)
N(9)	2587(4)	11088(3)	6286(3)	26(1)	O(26)	6788(9)	10681(7)	14871(6)	151(4)
N(10)	3620(6)	12679(3)	6517(3)	42(2)	O(27)	6457(7)	11264(4)	7063(4)	95(3)
Ni(1)	8102(1)	6180(1)	3284(1)	22(1)	O(28)	1448(6)	12904(4)	6265(4)	79(2)
Ni(2)	8995(1)	10079(1)	6451(1)	25(1)	P(1)	6771(1)	5153(1)	5211(1)	14(1)
O(1)	7834(3)	5202(2)	5661(2)	17(1)	P(2)	6627(1)	4799(1)	7315(1)	16(1)
O(2)	6552(3)	4322(2)	5037(2)	19(1)	C(1)	7318(9)	7664(6)	4319(6)	75(3)
O(3)	5842(3)	5420(2)	5718(2)	20(1)	C(2)	6629(10)	7438(6)	3727(7)	97(4)
O(4)	6835(4)	5614(2)	4495(2)	21(1)	C(3)	10424(6)	6344(4)	3567(5)	43(2)
O(5)	6824(4)	5626(2)	7059(2)	19(1)	C(4)	10305(7)	6098(6)	4357(5)	57(2)
O(6)	7150(3)	4249(2)	6751(2)	18(1)	C(5)	8669(11)	8500(5)	6855(5)	69(3)
O(7)	5444(3)	4636(2)	7296(2)	20(1)	C(6)	8672(12)	8502(5)	6053(5)	85(4)
O(8)	7087(3)	4697(2)	8094(2)	19(1)	C(7)	9184(9)	11686(5)	6838(5)	59(3)
O(9)	8904(4)	5148(2)	6868(2)	23(1)	C(8)	8949(10)	11671(5)	6051(5)	65(3)
O(10)	7944(3)	3485(2)	5744(2)	23(1)	C(9)	3682(6)	11331(4)	6102(4)	33(2)
O(11)	5076(3)	3877(2)	6049(2)	23(1)	C(10)	3790(7)	12151(4)	5882(4)	41(2)
O(12)	4542(4)	5809(2)	6696(2)	25(1)					

$U(\text{eq})$  is defined as one third of the trace of the orthogonalized  $U_{ij}$  tensor.

Table 5. BVS values for Mo, P and Ni in **1**.

Cation	BVS	Cation	BVS	Cation	BVS
Mo(1)	5.990	Mo(4)	6.057	P(2)	4.987
Mo(2)	5.976	Mo(5)	6.137	Ni(1)	2.093
Mo(3)	5.983	P(1)	4.894	Ni(2)	2.134

and refinement statistics for **1** are listed in table 1. Selected bond distances and angles are given in tables 2 and 3, respectively. Final atomic coordinates and thermal parameters are listed in table 4.

### 2.3. Bond valence sum calculation

The concept of bond valence sum (BVS) [8] is important in solving crystal structures of many new materials. Bond valence (S) correlates with the bond length (R) through a relationship which can be expressed as  $S = \exp(R_0 - R)/B$ , where R is the experimentally determined interatomic distance and  $R_0$  and B are constants depending on the atoms [9]. BVS values of the cations in **1** are tabulated in table 5. The table shows that average values of calculated oxidation states are 6.029 for Mo, 4.941 for P and 2.114 for

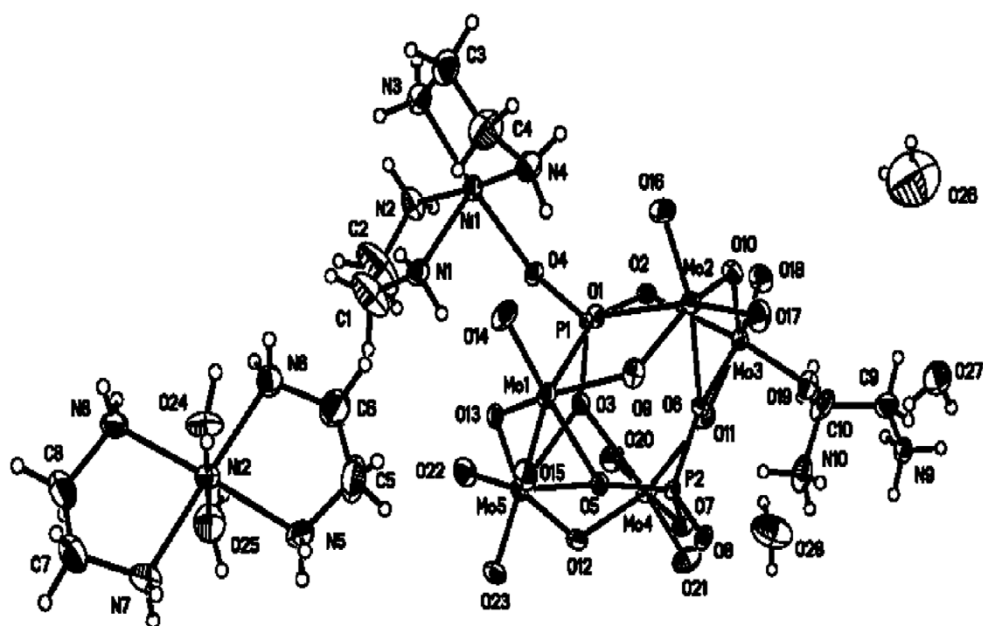


Figure 1. Structure of the compound **1** and its atomic numbering scheme.

Ni, consistent with formula of **1**. The rationality of the crystal structure was proven by BVS values indirectly.

### 3. Results and discussion

#### 3.1. Structure description

As seen in figure 1, there are two different types of  $[\text{Ni}(\text{en})_2]$  fragments in **1**. The first consists of  $[\text{Ni}(1)(\text{en})_2(\text{PO}_4)_2\text{Mo}_5\text{O}_{15}]^{4-}$  anions, in which each octahedrally coordinated nickel atom bridges two  $[(\text{PO}_4)_2\text{Mo}_5\text{O}_{15}]^{6-}$  clusters. The Ni(1) site is defined by four nitrogen donors from two en molecules and two *trans* oxo atoms of adjacent  $[(\text{PO}_4)_2\text{Mo}_5\text{O}_{15}]^{6-}$  clusters with Ni(1)–O(4) and Ni(1)–O(8) distances 2.090(4) and 2.198(4) Å, respectively. Ni(1)–N distances are in the range of 2.083(6)–2.113(6) Å.  $[\text{Ni}(2)(\text{en})_2(\text{H}_2\text{O})_2]^{2+}$  ions occupy regions between adjacent sinusoidal layers acting as a charge-compensating component. The Ni(2) site has Ni(2)–N distances in the range of 2.075(6)–2.108(6) Å. In contrast to the bridging  $[\text{Ni}(1)(\text{en})_2]^{2+}$  groups, nickel atoms of the second group exhibit only weak interactions with the  $[(\text{PO}_4)_2\text{Mo}_5\text{O}_{15}]^{6-}$  clusters and have strong covalent attachments to  $\text{H}_2\text{O}$  molecules with Ni(2)–O(24) and Ni(2)–O(25) distances of 2.090(5) and 2.141(5) Å, respectively.

Thus the structure of **1** is constructed by the linking of  $[(\text{PO}_4)_2\text{Mo}_5\text{O}_{15}]^{6-}$  clusters and  $[\text{Ni}(\text{en})_2\text{O}_2]^{2+}$  octahedra into spiral chains of  $[\text{Ni}(\text{en})_2(\text{PO}_4)_2\text{Mo}_5\text{O}_{15}]^{4-}$  ions as shown in figure 2. The  $[(\text{PO}_4)_2\text{Mo}_5\text{O}_{15}]^{6-}$  clusters are constructed from  $\text{MoO}_6$  octahedra and  $\text{PO}_4$  tetrahedra. Five distorted  $\text{MoO}_6$  octahedra aggregate in a compact edge- or

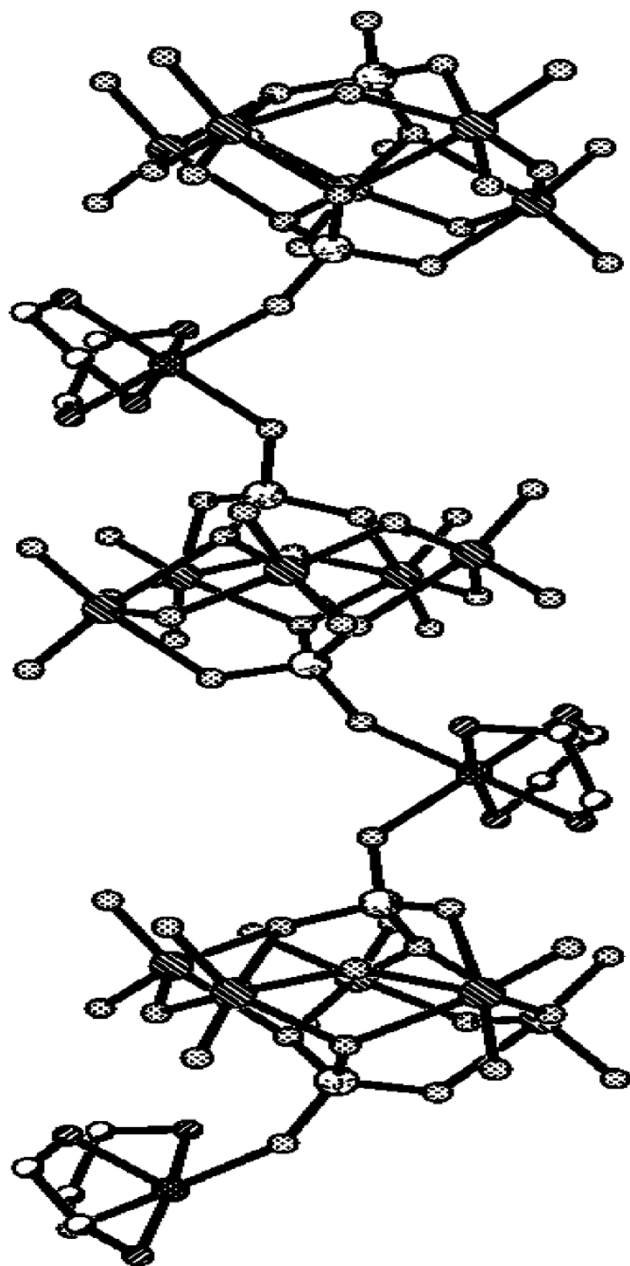


Figure 2. Structure of the  $[\text{Ni}(\text{en})_2(\text{PO}_4)_2\text{Mo}_5\text{O}_{15}]^{4-}$  chains.

corner-sharing arrangement in a plane to form a ring with two  $\text{PO}_4$  tetrahedra capped above and below the ring. The Mo(1)–, Mo(2)–, Mo(3)–, Mo(4)–, and Mo(5)–O distances are 1.709(5)–2.309(4), 1.712(5)–2.358(4), 1.706(4)–2.362(4), 1.704(5)–2.478(4) and 1.699(5)–2.348(4) Å, respectively. P(1)–O and P(2)–O distances are in the ranges 1.524(4)–1.564(4) and 1.516(5)–1.552(4) Å, respectively. Two adjacent



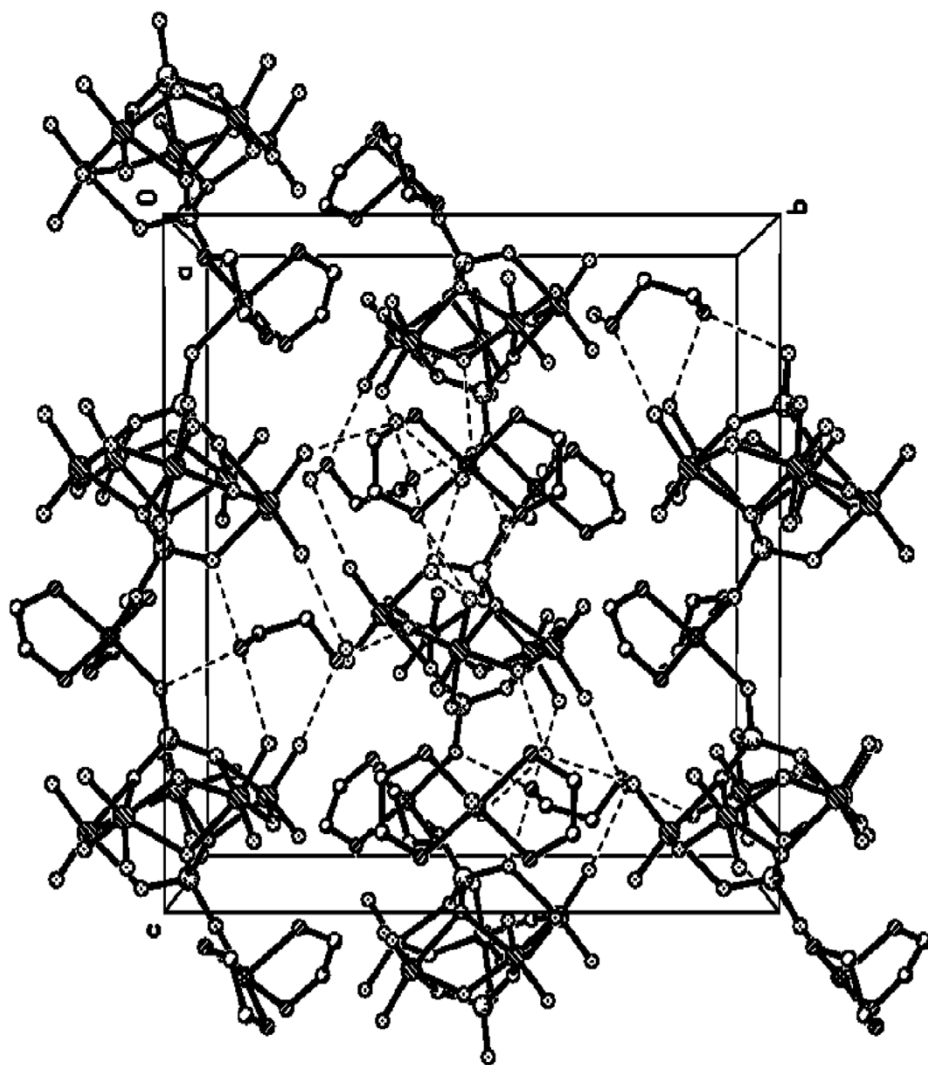


Figure 3. Packing diagram of 1.

$[(\text{PO}_4)_2\text{Mo}_5\text{O}_{15}]^{6-}$  clusters are connected through a  $[\text{Ni}(\text{en})_2]^{2+}$  unit *via* corner-sharing interactions of the type  $\text{PO}-\text{Ni}(1)$  with  $\text{P}(2)-\text{O}(8)-\text{Ni}(1)$  and  $\text{P}(1)-\text{O}(4)-\text{Ni}(1)$  angles of  $130.7(2)$  and  $135.8(3)^\circ$ ; the  $\text{Ni}(1)-\text{O}(4)$  distance of  $2.090(4)$  Å is shorter than  $\text{Ni}(1)-\text{O}(8)$  ( $2.198(4)$  Å). Figure 3 shows that  $[\text{Ni}(\text{en})_2(\text{PO}_4)_2\text{Mo}_5\text{O}_{15}]^{4-}$  chains are parallel and packed in such a way that each chain is circumscribed by two groups of four similar chains related by a *pseudo* 4-fold axis. The infinite 1-D chains are connected by hydrogen bonds between oxygen atoms of anions and nitrogen atoms of en molecules to form a layer (table 6). Within the layer lie irregular tunnels occupied by  $\text{H}_2\text{O}$  molecules and the charge-compensating  $[\text{Ni}(\text{en})_2(\text{H}_2\text{O})_2]^{2+}$  and  $(\text{H}_2\text{en})^{2+}$  cations.



Table 6. Hydrogen bond details (Å).

D...A	d(D...A)	D...A	d(D...A)
N1...O13	3.017	N9...O2 [x-1/2, -y+3/2, -z+1]	2.806
N1...O22 [x+1/2, -y+3/2, -z+1]	3.113	N9...O15 [-x+1, y+1/2, -z+3/2]	2.947
N2...O17 [-x+3/2, -y+1, z-1/2]	3.092	N10...O11 [x, y+1, z]	2.923
N3...O7 [-x+3/2, -y+1, z-1/2]	2.875	N10...O21 [x, y+1, z]	3.167
N3...O19 [-x+3/2, -y+1, z-1/2]	3.343	N10...O23 [-x+1, y+1/2, -z+3/2]	2.806
N3...O23 [x+1/2, -y+3/2, -z+1]	2.985	N10...O28	2.799
N3...O22 [x+1/2, -y+3/2, -z+1]	3.166	O24...O4 [x+1/2, -y+3/2, -z+1]	2.757
N4...O1	2.981	O24...O9 [-x+2, y+1/2, -z+3/2]	2.760
N4...O14	3.107	O24...O8 [-x+2, y+1/2, -z+3/2]	2.959
N4...O16	3.125	O25...O27	2.680
N5...O17 [-x+2, y+1/2, -z+3/2]	3.118	O25...O26 [x, y, z-1]	2.696
N5...O21 [-x+1, y+1/2, -z+3/2]	3.005	O26...O16 [x-1/2, -y+3/2, -z+2]	2.735
N6...O20 [x+1/2, -y+3/2, -z+1]	2.876	O26...O28 [x+1/2, -y+5/2, -z+2]	3.257
N6...O4 [x+1/2, -y+3/2, -z+1]	3.480	O26...O20 [x+1/2, -y+3/2, -z+2]	2.727
N7...O27	3.136	O27...O19 [x, y+1, z]	2.793
N8...O2 [x+1/2, -y+3/2, -z+1]	3.191	O27...O12 [-x+1, y+1/2, -z+3/2]	2.682
N8...O20 [x+1/2, -y+3/2, -z+1]	2.940	O28...O17 [x-1, y+1, z]	3.163
N9...O8 [-x+1, y+1/2, -z+3/2]	2.731	O28...O18 [x-1/2, -y+3/2, -z+1]	2.852

### 3.2. IR spectroscopy and TG-DTA analysis

FT-IR spectra of **1** exhibit bands at 2945, 1590, 1458, 1326 and 1278  $\text{cm}^{-1}$ , characteristic of en. Bands at 1090 and 1032  $\text{cm}^{-1}$  can be assigned to P–O stretching and bands at 980, 948, 908 and 889  $\text{cm}^{-1}$  to  $\nu(\text{Mo}=\text{O})$  and  $\nu(\text{Mo}-\text{O}-\text{Mo})$ . Ni–N stretches are assigned to 277, 342 and 401  $\text{cm}^{-1}$  [10]. Lattice water absorbs at 3426, 3348 and 3301  $\text{cm}^{-1}$  (antisymmetric and symmetric modes). Coordinated water absorbs at 680, 565 and 504  $\text{cm}^{-1}$  ( $\rho_{\text{r}}(\text{H}_2\text{O})$ ,  $\rho_{\text{w}}(\text{H}_2\text{O})$  and  $\nu(\text{NiO})$ , respectively) [11].

The thermal stability of **1** was examined TGA-DTA in dry air at a heating rate of 5°C  $\text{min}^{-1}$  from room temperature to 850°C. The TG curve indicates that weight loss can be divided into five distinct stages. Below 150°C, weight loss of 6.4% with an endothermic peak corresponds to the successive release of coordinated and crystalline water in good agreement with the calculated value (6.34%). Weight loss of 13.0% (calculated 12.82%) observed from 150 to ca 410°C is attributed to the release of en from  $[\text{Ni}(2)(\text{en})_2(\text{H}_2\text{O})_2]^{2+}$  and  $(\text{H}_2\text{en})^{2+}$ . Two exothermic peaks, with a weight loss of 20.1% (calculated 20.48%), were observed in the temperature range 450 to 600°C, and these are ascribed to decomposition of the  $[\text{Ni}(1)(\text{en})_2(\text{PO}_4)_2\text{Mo}_5\text{O}_{15}]^{4-}$  chains to  $\text{MoO}_3$ ,  $\text{P}_2\text{O}_5$  and  $\text{NiO}$ . With increasing temperature, an obvious exothermic peak at 636°C and a low weight gain were found, indicating chemical reaction among metal oxides to form an unknown phase that is unstable, losing weight above 700°C.

### Supplementary data

Crystallographic data have been deposited with the Cambridge Crystallographic Data Centre as supplementary publication CCDC 295867. Copies of the data may be obtained free of charge on application to CCDC, 12 Union Road, Cambridge

CB2 1EZ, UK (Fax: +44 1223 336033; E-mail: deposit@ccdc.cam.ac.uk or www: http://www.ccdc.cam.ac.uk).

## Acknowledgement

This work was supported by the Doctoral Foundation of Jinan University.

## References

- [1] M.T. Pope. *Heteropoly and Isopoly Oxometalates*, Springer-Verlag, Berlin (1983).
- [2] M.T. Pope, A. Muller. *Polyoxometalates: From Platonic Solids to Anti-Retroviral Activity*, Kluwer Academic Publishers, Dordrecht, The Netherlands (1994).
- [3] Y.P. Jeannin. *Chem. Rev.*, **98**, 51 (1998).
- [4] J.Y. Niu, M.L. Wei, J.P. Wang, D.B. Dang. *Eur. J. Inorg. Chem.*, 160 (2004).
- [5] P. Mialane, A. Dolbecq, L. Lisnard, A. Mallard. *Angew. Chem. Int. Ed.*, **41**, 2398 (2002).
- [6] U. Kortz, J. Vaissermann, R. Thouvenot, P. Gouzerh. *Inorg. Chem.*, **42**, 1135 (2003).
- [7] *SAINTE* and *SADABS*, Bruker Analytical X-ray Systems, Inc., Madison, WI, USA (1998).
- [8] I.D. Brown. *Acta. Cryst.*, **B33**, 1305 (1977).
- [9] C. Hormillosa, S. Healy, T. Stephen. *Bond Valence Calculator, Version 2.0*, McMaster University, Ontario, Canada (1993).
- [10] A.B.P. Lever, E. Mantovani. *Can. J. Chem.*, **51**, 1567 (1973).
- [11] K. Nakamoto. *Infrared and Raman Spectra of Inorganic and Coordination Compounds*, pp. 228–229, John Wiley and Sons, New York (1986).